

# LCAO TRUNCATED CRYSTAL CALCULATIONS ON SOME ELECTRONIC PROPERTIES OF COMPRESSED MOLECULAR HYDROGEN CRYSTAL

ALEX ZUNGER

Department of Theoretical Physics, Soreq Nuclear Research Centre, Yavne, Israel and Department of Chemistry, Tel Aviv University, Tel Aviv, Israel

(Received 15 October 1973)

**Abstract**—The truncated crystal method is used to describe the band gap, work function, repulsive ground state crystal potential, Davydov excitons and defect states due to H and N<sub>2</sub> impurities, in molecular Pa3 hydrogen crystal, utilizing a simplified minimal basis set and semiempirical quantum chemical methods. Favorable results are achieved regarding experimental optical data.

## 1. INTRODUCTION

The truncated crystal approach to the description of electronic properties of covalent solids, has been successfully applied in recent years to a large variety of problems[1-6]. This method, characterized by solving for the eigenvalues of a finite cluster of atoms either by LCAO representation or by Slater's X $\alpha$  method[7] and seeking convergence of some properties as a function of cluster size, when the conditions imposed on the boundaries are either periodic connections[5, 8, 9] or chemical substitution satisfying the valence of the dangling bonds[2], has proved to be useful in several respects:

(1) when convergence limit is reached, it is possible to describe localized point defect states as well as electronic states of the infinite ideal crystal by the same method, thereby providing an intermediate scheme between band theory[10] and defect molecule[11] approaches to the defect problem.

(2) the use of charge iterative SCF-LCAO methods accounting for charge redistribution between the atoms forming the cluster, permits calculation both as a function of density and of properties of clusters where a guest atom or molecule with different electronegativity than the host crystal, has been substituted[5].

These advantages of the truncated crystal approach are used in this paper to calculate various electronic properties of molecular hydrogen crystals.

Much theoretical effort has been devoted lately to the investigation of properties of compressed solid hydrogen at low temperatures, mainly due to the interesting possibility of producing a high pressure phase of metallic

hydrogen in the laboratory[12, 14], and because of interest in laser production of hydrogen plasma from cold solid hydrogen, for use in thermonuclear reactions[15]. The former problem, treated from the point of view of metal-insulator transition, requires the knowledge of the equation of state[16, 17] and also the variation of one-electron energy states in the molecular phase with density[13]. The latter phenomenon, involving in its first stage bound-bound absorption processes of photons at optical frequencies by the cold solid hydrogen, which is a high band gap insulator ( $E_g \sim 11$  eV), offers likewise questions involving the density dependence of electronic properties, namely: to what extent it is possible to lower the ionization potential and the lowest singlet-singlet excitation energy (band gap) of the solid (which are both much higher than the energy of the photons impinged on it) by increasing its density. Another practical approach suggested to lower the energy of the first electronic transition, to a conducting state is to introduce simple impurities (H, N<sub>2</sub>, etc.) into the molecular solid, thereby creating states in the gap. In this connection it is interesting to inquire into the nature at these impurity states and their separation from the bottom of the conduction band.

In Section 2 we describe the molecular cluster method and specify the quantum mechanical methods that are used with it. In Section 3 we treat some one-electron states in the crystal (corresponding to energies of ionization and edge of conduction band) and in Section 4 the Frenkel exciton states are discussed by the same method. In Section 5 we present some model calculations on impurity states in solid hydrogen.

## 2. DESCRIPTION OF THE MOLECULAR CLUSTER MODEL

The electronic wave functions of a crystal in the LCAO approach are given by:

$$\phi_i = \sum_{\nu=1}^N C_{i\nu} \chi_{\nu} \quad i = 1, 2, \dots, N \quad (1)$$

where  $\chi_{\nu}$  denote the atomic orbitals on site  $\nu$ . The  $C_{i\nu}$  are the solutions to the one-electron Hartree-Fock equations for the crystal, given by:

$$\sum_{\nu=1}^N (F_{\mu\nu} - S_{\mu\nu} \epsilon_i) C_{i\nu} = 0 \quad i = 1, 2, \dots, N. \quad (2)$$

The  $\epsilon_i$  are the one-electron crystal orbital energies,  $F_{\mu\nu}$  are the matrix elements of the one-electron effective Hamiltonian in the frame of the atomic orbitals and  $S_{\mu\nu}$  are overlap integrals between these atomic orbitals. We are interested in the solutions of (2) both for the case of a defect placed in the crystal, and for the crystal maintaining perfect translational symmetry. We would also be interested in correlating the properties of the crystal orbitals belonging to the localized defect state with states of the ideal crystal. Therefore, instead of factorizing the secular problem (2) by considering translational symmetry, we propose to solve (2) directly under some simplifying assumptions on  $F_{\mu\nu}$ , as a function of  $N$ , for known crystal symmetry, and to examine the convergence of some electronic properties both of the ideal cluster and the one perturbed by a point defect, as  $N$  is increased. The convergence of each property is examined for various densities, through a charge self-consistent solution of (2), thereby providing a simple density description of these properties. This truncated crystal approach was previously applied to lattice dynamic properties of atomic solids [18, 19] and to electronic properties of atomic [1-6] and molecular [20] solids.

The matrix elements  $F_{\mu\nu}$  are approximated either by the Cusacks approximation [21, 22] or by the SCF-LCAO INDO approximation [23]. In the former case, the off diagonal matrix element are given by:

$$F_{\mu\nu} = S_{\mu\nu} [H_{\mu\mu}(Q_{\mu}) + H_{\nu\nu}(Q_{\nu})] \times (1 - 0.5 |S_{\mu\nu}|) \quad (3)$$

where the diagonal elements are taken to be charge dependent through the relation

$$H_{\mu\mu}(Q_{\mu}) = H_{\mu\mu}^0 + Q_{\mu} \Delta_{\mu} \quad (4)$$

and  $H_{\mu\mu}^0$  is the Hartree-Fock free atom one-electron orbital energy for the  $\mu$ th orbital, and  $\Delta_{\mu}$  is the change in orbital energy per unit charge. A minimal basis set of Slater orbitals is employed. For hydrogen 1s state,  $H_{\mu\mu}^0$  is

taken as  $-13.6$  eV and  $\Delta_{\mu}$  as  $-14.0$  eV [22].  $S_{\mu\nu}$  are calculated using Slater orbitals with the best variational exponent of 1.2. After obtaining an initial guess for the charges  $Q_{\mu}$  for all atoms, the matrices  $S_{\mu\nu}$  and  $F_{\mu\nu}$  are constructed and equation (2) solved for a chosen  $N$  assuming the experimental  $Pa3$  structure. The clusters are formed by taking a central molecule and adding successive shells of neighbours (13, 18, 43, 55, 77 molecules for 1, 2, 3, 4, 5 orders of neighbours, respectively). Since we are not interested in the properties of the small clusters themselves, the intermolecular distances are taken to be the bulk values with no relaxations allowed. The coefficients  $C_{i\nu}$  are then used to calculate the net atomic charges  $Q_{\mu}$  for all the atoms and the cycle repeated until convergence of  $0.005 e$  is obtained between successive iterations. The atomic charges are computed from one and two center contributions to the charge moments by a procedure that leaves the projection of the centroid of charge, onto the line connecting the two atoms, unchanged [22]. This avoids the usual procedure of dividing the bond charge equally between the atoms involved, a procedure that yields erroneous results when the atoms involved have different electronegativities.

The one-electron energy levels obtained, are populated with  $N$  electrons and the band gap is defined as the difference between highest occupied and lowest vacant cluster states, while the Koopman's cluster ionization potential is taken as the negative of the energy of the highest occupied state. The derivation of the Mulliken approximation for the off diagonal matrix element  $F_{\mu\nu}$ , closely related to the Cusacks approximation employed here from Hartree-Fock equations [24, 25], shows that for systems with relatively homogeneous charge distribution, this method provides a reasonable approximation. In the limit of an isolated  $H_2$  molecule, at experimental equilibrium internuclear separation, this procedure yields a ionization potential of 15.38 eV compared with the experimental [26] value of 15.43 eV, an  $X^1\Sigma_g$  to  $B^1\Sigma_u$  one-electron energy gap of 10.965 eV as compared with the experimental value of 11.18 eV [26], while the dissociation energy calculated by this method yields a value of 4.66 eV as compared with the experimental value of 4.474 eV [26].

In the INDO approach, the off diagonal matrix element is taken as

$$F_{\mu\nu} = \beta_{AB}^0 S_{\mu\nu} - \frac{1}{2} P_{\mu\nu} \gamma_{AB} \quad (5)$$

and the diagonal elements are

$$F_{\mu\mu} = U_{\mu\mu} + (P_{AA} - \frac{1}{2} P_{\mu\mu}) \gamma_{AA} + \sum_{B \neq A} (P_{BB} \gamma_{AB} - V_{AB}) \quad (6)$$

where the bonding parameter  $\beta_{AB}^0$  is determined empiri-

cally to give an overall best fit to accurate LCAO-SCF calculations for diatomics[23],  $P_{\mu\nu}$  is the bond order matrix,  $P_{AA}$  and  $P_{BB}$  are total charge density on atoms  $A$  and  $B$  respectively and  $\gamma_{AB}$  and  $\gamma_{AA}$  are electron repulsion integrals calculated directly. The core Hamiltonian element  $U_{\mu\mu}$  is taken as  $-13.06$  eV while the interaction element of an electron on atom  $A$  with the core of atom  $B$ ,  $V_{AB}$ , is calculated according to formulas given by Roothaan[27]. When the electron repulsion integrals are not parametrized, the agreement for  $H_2$  properties with experiment is quite poor[23]. We followed the original formulation (equations 5-6) of Pople *et al.*[23], and used the INDO approach in truncated crystal calculation only to a limited extent, due to its failure to account reasonably for the free molecule properties (although different parametrization schemes could produce a better agreement).

### 3. BAND GAP AND IONIZATION POTENTIAL IN SOLID $Pa_3$ HYDROGEN

Figure 1 represents the calculated band gap and ionization potential for  $Pa_3$  clusters of increasing number of molecules as obtained in the truncated crystal calculations with IEXH calculations. For 3 orders of neighbours, convergence is obtained even for the highest density considered ( $V = 9.6$  cm<sup>3</sup>/mole). The band gap (defined here as the difference between lowest vacant and highest occupied crystal orbital energies) and ionization potential are shown to decrease from their free molecule values, due to band structure effects, as molecules are accumulated to form clusters, and further decrease is obtained as the density increases. Since the relatively delocalized empty band is probably not adequately described by the minimal basis set employed, and since this description becomes even poorer as the conduction band approaches the valence band, no attempt was made to further increase the density of the cluster towards the metal hydrogen limit.

The convergence of the band gap and ionization potential as a function of cluster size, as obtained by applying the INDO approximation to the matrix elements in equations (5-6), is shown in Fig. 2. Since this procedure, as already noted, yields poor agreement even with isolated molecule experimental data for these properties, the values obtained for cluster calculation are not of much interest, and we will proceed with the IEXH approximations to further discuss cluster properties. It is however worth mentioning that the relative decrease in ionization potential and band gap, as a function of cluster size, is similar in both methods, indicating that cluster models of this size are probably sufficient to describe these properties in the bulk.

Since the charge distribution over the atoms in the molecular cluster was relatively homogeneous even at the clusters surface (contrary to the situation in clusters

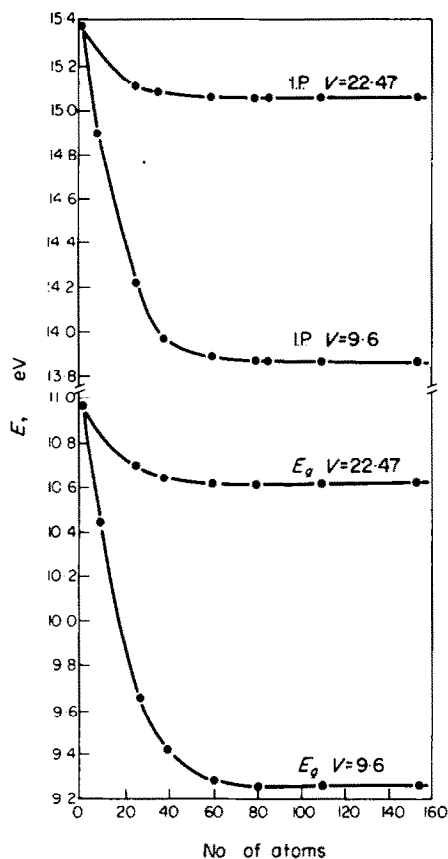


Fig. 1. Variation of ionization potential (I.P.) and band gap ( $E_g$ ) with cluster size for two volumes ( $V$  in cm<sup>3</sup>/mole) as calculated for IEXH clusters.

representing atomic solids such as graphite[5b], boron nitride[5a] and diamond[2, 4] where the bonded atomic interactions tend to accumulate excess charge on the unsaturated atoms at the surface), no attempt has been made to apply periodic boundary conditions to suppress charge inhomogeneity. This however would probably be important in similar studies on atomic hydrogen crystals[28].

In Fig. 3, the density dependence of some calculated electronic properties of solid  $Pa_3$  hydrogen is revealed, as obtained in the cluster calculation with IEXH approximation. The limiting values obtained for low densities corresponding to the free molecule values, coincide with the values obtained by the same method of calculation for a single molecule. For the experimental equilibrium volume ( $V = 22.47$  cm<sup>3</sup>/mole,  $a = 5.2875$  Å) the band gap in the cluster is 10.7 eV, as compared with the lower edge of the singlet-singlet absorption of solid  $D_2$  obtained by Baldini[29] in the u.v. spectrum, of 10.8 eV. For the highest density considered ( $V = 9.6$  cm<sup>3</sup>/mole), the gap

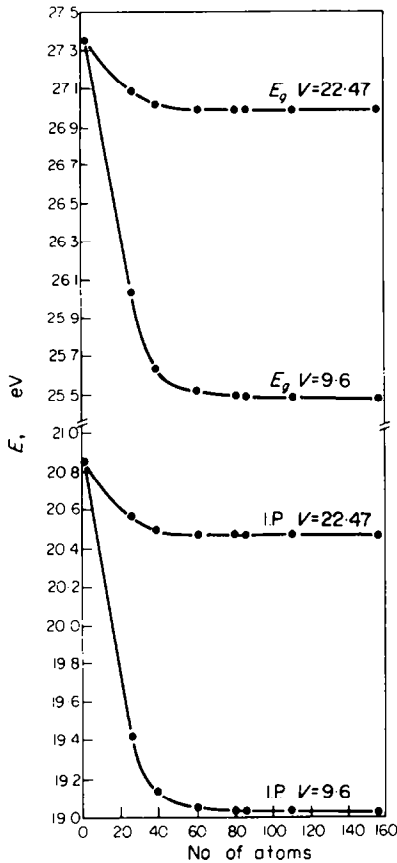


Fig. 2. Variation of ionization potential (*I.P.*) and band gap ( $E_g$ ) with cluster size for two volumes ( $V$  in  $\text{cm}^3/\text{mole}$ ) as calculated for INDO clusters.

decreases to 9.2 eV\*. It is also observed that the decrease in the band gap is mainly due to the decrease of the energy of the upper edge of the valence band with density while the edge of the first empty band is only slightly affected by density. The width of the valence band is 1.22 eV at equilibrium volume and rises to 4.94 eV at  $V = 9.6 \text{ cm}^3/\text{mole}$ .

An attempt to calculate electronic energy changes in solid molecular hydrogen due to density changes, was previously made by Chapline[13]. The change in one-electron energy from that in a hydrogen molecule was determined by a Wigner-Seitz model, considering the first order perturbation contribution due to the electronic wave function outside the molecular Wigner-Seitz sphere. Extending this calculation to lower densities, shows that the Wigner-Seitz model results in one-electron energies

\*This decrease in excitation energy upon compression is probably too low for increasing significantly the absorption efficiency of Neodimium laser photons ( $h\nu = 1.17 \text{ eV}$ ) by cold and compressed hydrogen targets via bound-bound absorption mechanisms, in experiments of laser produced plasma.

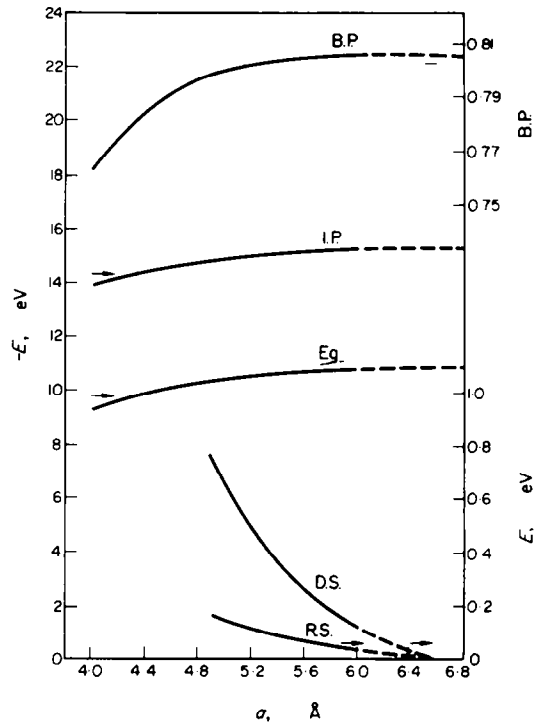


Fig. 3. Density dependence of several electronic properties at the convergence limit, calculated by IEXH method. *B.P.*: bond population, *I.P.*: ionization potential,  $E_g$ : band gap, *D.S.*: Davydov splitting, *R.S.*: Red shift of the center of the band.

that are lower than those obtained by the molecular cluster approximation, reaching at the limit of very low density to an overestimation of 5–6 eV of the experimental ionization potential. This large deviation both from experimental results at very low densities and from the cluster model at intermediate densities would probably have a large effect on the point of energy crossing obtained with the Wigner-Seitz model for molecular and metallic forms[13, 14].

The binding energy per molecule, is calculated in the cluster model by summing the one-electron energy levels of all occupied states. Since LCAO treatment of closed shell systems reveals only the repulsive potential[30, 31] (unless configuration interaction is introduced), the excess energy per molecule as compared to the free molecule, is positive. Comparing the results for this interaction energy of our cluster calculation with the phenomenological form of pair interaction

$$\phi_{rep} = 4\epsilon \left(\frac{\sigma}{r}\right)^{12} \quad (7)$$

we get for  $3.70 \text{ \AA} < r < 3.80 \text{ \AA}$ , taking the accepted value of  $N\sigma^3 = 15.6 \text{ cm}^3$ [32] a value of  $\epsilon \sim 43^\circ\text{K}$  for the 77 molecule cluster, and  $\epsilon \sim 42^\circ\text{K}$  for the 55 molecule cluster,

as compared with the experimental value of the bulk crystal of 36.7°K deduced from compressibility and second virial coefficient data[32]. Reasonable agreement between the repulsive part of the phenomenological interaction potential and that calculated from LCAO cluster approximation, was previously obtained also for  $N_2-N_2$  interaction[20].

A different representation of the interaction in the crystal could be obtained by calculating the change in bond population[22] of the central molecule in the cluster, versus cluster density (Fig. 3). This population, describes the strength of the molecular bond at various crystal densities. It is evident that upon compression of the unit cell, keeping the molecular bond length constant, this bond is weakened due to extraction of electronic charge from the region between two bonded hydrogen atoms. Such a behaviour was previously postulated for description of metal-insulator transitions due to destruction of diatomic bonds by pressure[33, 34].

#### 4. FRENKEL EXCITONS IN HYDROGEN $Pa3$ CRYSTAL

We next consider the energies of the Frenkel exciton states in molecular solid hydrogen by the same LCAO approach.

The low temperature  $Pa3$  ordered phase of hydrogen crystal has 4 molecules per unit cell and belongs to the  $T_{6h}$  factor group. A group theoretical analysis reveals that the free molecule (point group  $D_{2h}$ ) ground state  $^1\Sigma_{1g}$  yields in the  $T_{6h}$  factor group a totally symmetric representation  $A_{1g}$ , while the lowest free molecule singlet excited state  $B^1\Sigma_{1u}$  ( $1\sigma_g, 1\sigma_u$ ) state gives rise to a  $T_u + A_u$  representation in the factor group. The  $A_u$  state is optically inactive, while the transition to the triply degenerate  $T_u$  state is dipole allowed and polarized along the  $x, y, z$  unit cell directions. The transition to the free molecule zero vibrational state of  $B^1\Sigma_{1u}$  occurs at 11.235 eV[26] and at 11.181 eV in  $D_2$  and  $H_2$  respectively. The crystal spectrum of solid  $D_2$  at 6°K[29] reveals an absorption edge at 10.8 eV originating from the same molecular transition, followed by a relatively broad absorption band peaking at about 12 eV. At higher energies this absorption overlaps with the lower part of the  $2p^1\Pi_u$  absorption. The energy loss spectrum of solid  $H_2$  in the range of 11–16 eV was measured by Schmidt, and exhibits similar behaviour[35].

Denoting the wave function of the molecule occupying site  $i$  of unit cell  $n$  ( $i = 1, 2, 3, 4, n = 1, 2, \dots, N$ ) by  $\phi_{ni}^s$  and  $\phi_{ni}^o$  for the lowest excited singlet and the ground electronic state respectively, a straight forward Frenkel formalism yields for the  $Pa3$  group, the energies of the exciton states at  $\vec{K} = 0$  relative to the crystal ground state, as

$$\Delta E_{\lambda}^i = \Delta \epsilon^i + D^i + L_{ni,01}^i + \left( \frac{2}{3} L_{n2,01}^i + \frac{1}{3} L_{n3,01}^i + \frac{1}{3} L_{n4,01}^i \right) \quad (8)$$

where

$$L_{ni,01}^i = \sum_n \langle \phi_{ni}^s \phi_{01}^o | V_{ni,01} | \phi_{ni}^o \phi_{01}^s \rangle = \sum_n I_{ni}^i \quad (9)$$

$$D^i = \sum_n \langle \phi_m^s \phi_n^o | V_{mn} | \phi_m^o \phi_n^s \rangle - \langle \phi_m^o \phi_n^o | V_{m,n} | \phi_m^o \phi_n^o \rangle \quad (10)$$

$\Delta \epsilon^i$  is the free molecule excitation energy to state  $s$  and  $V_{ni,mi}$  is the intermolecular potential (in equation 10 the double indices are suppressed). Molecule 1 at the origin of the unit cell was chosen as a reference. The state with  $\lambda = 1$  is of  $A_u$  symmetry while the states  $\lambda = 2, 3, 4$  belong to the triply degenerate  $T_u$  representation. Since for dipole allowed states in the  $Pa3$  structure, all  $L_{ni,01}$  are equal, we denote  $J' = L_{ni,01}$  for  $\lambda = 2, 3, 4$  and  $J = L_{n1,01}$ , adopting the notation of Hexter for vibrational excitons[36]. The splitting between the  $T_u$  and  $A_u$  states (Davydov splitting) is  $2J'$  while the shift of the center of the band relative to the free molecule transition is  $(D^i + J)$ .

The energies of the exciton states will be evaluated in two ways: (a) evaluation of the matrix elements  $L_{ni,01}^i$  from direct solution of the LCAO problem for  $H_2$  dimers oriented mutually as pairs in the crystal; (b) expansion of the  $L_{ni,01}^i$  matrix elements in multipole series and retention of the first non zero (dipole) term which could in turn be evaluated from the transition dipole to the free molecule excited state.

(a) The splitting between the excited states of a  $H_2$  dimer formed from molecules 1 and 2, is twice the summand in equation (9). These splittings are computed for  $H_2$  dimers oriented mutually as pairs in the  $Pa3$  structure, and the sum in equation (9) evaluated directly for  $n$  ranging to 6 orders of neighbours. The dimers one-electron energies are computed by IEXH method (equation 3) with the atomic parameters mentioned in Section 2. This yields at normal density, a splitting of 0.44 eV. The ground state Davydov splitting (between  $A_u$  and  $T_u$  states at  $\vec{K} = 0$ ) is similarly calculated to be 1.22 eV.

The additivity of pair interactions is checked, in the nearest neighbour approximation by comparing the splitting yielded by equation (9) when  $n$  is extended to nearest neighbours only, with the splitting obtained from the LCAO solution of one unit cell (4 molecules) weighted according to the number of neighbours. The results thus obtained agree with each other within 2%–4% in the density range between 22.47 cm<sup>3</sup>/mole and 17.5 cm<sup>3</sup>/mole. This is a measure for non additivity corrections in this model.

The first order contribution to the shift of the center of the band relative to the free molecule transition is computed both by summing pair interactions calculated for  $H_2$  dimers, according to equations (9) and (10) and by

performing a cluster calculation on one molecule surrounded by 5 orders of neighbours and analyzing the resultant one-electron energy levels to obtain the shift of the band. The result of the first calculation is  $-0.10$  eV while the cluster calculation reveals a shift at  $-0.093$  eV. Higher order perturbation terms corresponding to different polarizations of the crystal by the ground and excited state are difficult to calculate and could be important in determining the Davydov shift. The experimental shift of the center of the absorption band in  $D_2$ [29] is approximately  $0.05$  eV.

(b) A different approach to evaluate the energies of the dipole allowed exciton states rests upon expanding the interaction potential in multipole series and retaining only the first non zero moment. Equation (9) in this approximation becomes

$$L_{ni,01}^s = |M^s|^2 \sum_{\lambda} \frac{3 \cos \theta_{i\lambda} \cos \theta_{j\lambda}}{|R - r_{\lambda}|^3} \quad (11)$$

where  $R_{\lambda} = r_{\lambda} - R$  and  $R$  is the vector from a molecule on sublattice  $i$  to the nearest molecule on sublattice  $j$  and  $r_{\lambda} = \sum_i \lambda_i a_i$  is a lattice vector where  $a_i$  are unit cell vectors and  $\lambda$  are integers. If we denote the orientation of each sublattice by unit vectors  $\hat{e}_i$ , the angles are defined by:

$$\cos \theta = (\hat{e}_i \times \hat{e}_j) \quad \cos \theta_{i\lambda} = \frac{\hat{e}_i \times \hat{R}_{i\lambda}}{|\hat{R}_{i\lambda}|} \quad \cos \theta_{j\lambda} = \frac{\hat{e}_j \times \hat{R}_{j\lambda}}{|\hat{R}_{j\lambda}|} \quad (12)$$

and  $M^s$  is the molecular electronic transition dipole related to the absorption oscillator strength  $f$  by

$$|M^s|^2 = \frac{3he^2f}{8\pi^2m_e c \bar{\nu}} \quad (13)$$

where  $m_e$  is the electron mass and  $\bar{\nu}$  is the frequency at the center of the band. For an f.c.c. lattice, the sum in equation (11) can be easily evaluated by the Nijboer and de Wette procedure[37, 38]. Taking  $\bar{\nu}$  as the experimental frequency and  $f$  as the gas phase total oscillator strength  $0.28$ [39] and summing equation (11), we get as a splitting between  $A_u$  and  $T_u$  a value of  $0.15$  eV which is considerably lower than the value obtained by the LCAO cluster calculation, employing the full interaction. Splitting calculated according to dipole transition moments were shown in other cases to underestimate the experi-

mental value by a factor of 2-3, due to the neglect of other than dipole interactions and relaxation effects.\*

Mixing of the  $T_u$  exciton component with other  $T_u$  states originating from the free molecule dipole allowed  ${}^1\Pi_u$  state or the octupole allowed  ${}^1\Delta_u$  state are possible via second order crystal field effects, but will probably affect the splitting only to a small extent due to the large value of the oscillator strength to the  $B^1\Sigma_{1u}$  state.

When the calculation of the splitting in the semiempirical LCAO approach is performed for various crystal densities, it turns out that the splitting depends on the unit cell dimension  $a$  as  $a^{-8.1}$  (Fig. 3) over the range  $5.2 \leq a \leq 4.9$  Å, which is a much stronger dependence than that anticipated by pure dipole interactions. This short range character results from the description of intermolecular potential by overlap interactions[31] which fall quite rapidly with distance. Similarly, the Davydov splitting between the  $F_g$  states of the  $X^1\Sigma_g \rightarrow {}^1\Pi_g$  transition in  $\alpha$ -N<sub>2</sub> crystal, calculated by the same LCAO method[20] yielded a dependence of  $a^{-12.7}$  which is also much shorter range than the quadrupole  $a^{-5}$  potential usually employed to discuss this transition. It seems that both in  $\alpha$ -N<sub>2</sub> and in H<sub>2</sub>, the splittings discussed need to be considered by more general potentials, than the pure quadrupole and dipole potentials, respectively.

The number of pairs of states joining the valence and conduction levels respectively in the energy between  $h\omega$  and  $h\omega + hd\omega$ , are calculated from the one electron energy spectrum obtained for the largest molecular cluster considered. Since we treat finite clusters, only a histogram description is possible. Figure 4 describes this joint density of states, as obtained by sampling the clusters orbital energies. The edge of the absorption is now of  $T_u$  character and appears at  $10.5$ - $10.6$  eV as compared with the experimental value of Baldini[29] for D<sub>2</sub> crystal, of  $10.8$  eV. The region above  $\approx 11.3$  eV, is of  $A_u$  character and the transition to it is forbidden. The qualitative overall shape of the spectrum is similar to the observed absorption, though quantitatively the calculated spectrum is slightly narrower, probably due to the neglect of the atomic  $2p$  states that contribute to the high energy part of the spectrum.

The difference in ionization potential between an isolated H<sub>2</sub> molecule and the solid, was estimated from the electronic spectrum of large radius Wannier impurity states in  $X_n/H_2$  system[42] and in pure H<sub>2</sub>[43]. The impurity ionization potential in solid inert medium  $IP_m(s)$ , is related to the gas phase impurity ionization potential  $IP_m(g)$ , when the width of the hole state can be neglected, as in the case of Wannier type impurity states in doped solids, by the relation[44]:

$$IP_m(s) = IP_m(g) + P. + V., \quad (14)$$

where  $P.$  corresponds to the positive hole polarization

\*The overall splitting of the  $X^1\Sigma \rightarrow A^1\Pi$  transition in solid CO, calculated from the experimental oscillator strength[40] (not by the one postulated by Hexter[38]), yields in the dipole approximation a value of  $820$  cm<sup>-1</sup> as compared to experimental values of  $2500$  cm<sup>-1</sup>[41].

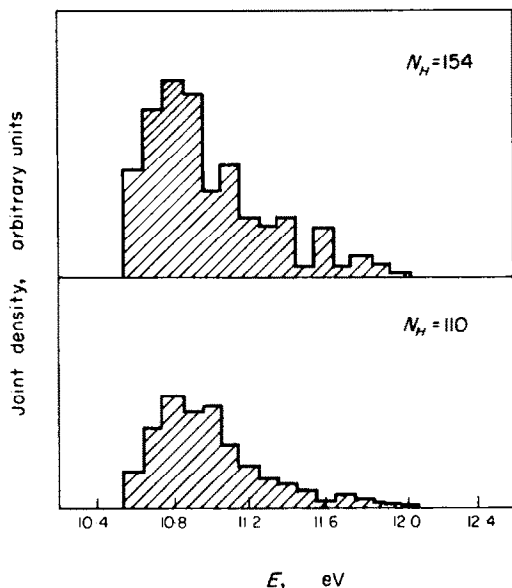


Fig. 4. Transition density of states (number of states connecting valence and conduction bands, respectively within energy range from  $E$  to  $E + \Delta E$ ) as a function of energy, as calculated by IEXH for the 110H and 154H clusters.

energy of the medium and  $V_0$  is the energy of the quasi free electron state corresponding to the bottom of the conduction state relative to the vacuum level. Similarly, the pure solid ionization potential  $IP(s)$ , is related to the ionization potential of its free constituents  $IP(g)$ , by [42]:

$$IP(s) = IP(g) + P_+ + V_0 + E_c \quad (15)$$

where  $E_c$  corresponds to the energy difference between the center of gravity and the upper edge of the valence band. Experimental determination of  $IP_m(s)$  for the  $X_n/H_2$  system [42] together with the knowledge of the experimental value of  $IP_m(g)$  for  $X_n$ , suggests that  $-(P_+ + V_0) \sim 1-2$  eV in solid  $H_2$ , which yields, through equation (15), taking  $IP(g) = 15.43$  eV [26], on a ionization potential for the solid of  $[13.5-14.5 + E_c]$  eV  $\approx 14.1-15.1$  eV. Evidence for a possible convergence limit of the Wannier series at 14.4 eV in pure solid  $H_2$  [43] suggests that  $IP(s) \sim 14.5$  eV should be a better guess.

Simple theoretical calculations of  $P_+$  [42] based on the Mott-Littleton [45] relation for static polarization energy and on charge-quadrupole interactions, yields  $P_+ \sim -0.8$  eV, while a simple pseudopotential calculation [40] yields  $V_0 = +2.2$  eV. This disagrees both with the value of  $V_0 \leq 0.5$  eV measured by Halpern and Gomer [47] for liquid  $H_2$ , and with the spectroscopic value of  $V_0 = -(1.2-0.2)$  eV, mainly due to the overestimation of the repulsive pseudopotential that was taken to depend semi-empirically on the scattering length.

## 5. POINT DEFECTS IN SOLID $H_2$

The relatively large band gap and ionization potential of solid  $H_2$  even at molar volumes as small as  $10$  cm<sup>3</sup>/mole, almost exclude processes such as simple bound optical transitions to conduction or ionized states, under conditions of irradiation with laser photons of energy in the range of 1-2 eV, as desired in experiments of laser heating of solid  $H_2$  [15, 48]. Multiphoton mechanisms [49] or generation of antistokes radiation inside the target [50] are not sufficient to enhance these absorption processes sufficiently. Another possible way of lowering the effective energy gap for such transitions, is introduction of impurities inside the solid target, thereby creating allowed electronic states in the otherwise forbidden gap. The truncated crystal method described in Section 2 was demonstrated to be suitable for calculation of such states in covalent crystals [2-6] because it provides a simple means of correlating the one-electron energy states of localized impurities with respect to the band edges. Employment of charge self-consistent methods to calculate the one-electron energy states of a cluster containing an impurity with different electronegativity than that of the host atoms, and the allowance made for small lattice distortions and relaxations around the center, provide useful mechanisms for introducing charge and energy redistribution effects that are important in problems of deep impurity states [4, 5].

We chose to discuss here some model calculations for two impurities that may enter unpurified solid hydrogen: an isolated hydrogen atom and a nitrogen molecule. The procedure of calculation goes in the following steps: (a) We choose a large enough hydrogen molecular cluster so that the examined (Section 3) electronic properties characterizing the bulk solid are already present in it. The molecular cluster of 43 molecules (1 central molecule at the origin + 3 shells) exhibits a band gap, ionization potential, average charge per atom and overlap population between two bonded atoms, very close to that of the convergence limit defined as that of the largest cluster considered (Fig. 1).

(b) The central  $H_2$  molecule at the origin is then replaced by the chosen impurity and the calculation of the new eigenvalues of the cluster, are repeated by increasing the cluster size from 3 to 4 and 5 shells of  $H_2$  molecules around the impurity, seeking convergence for the new one-electron levels.

(c) Once the one-electron energy levels associated with the impurity and the band edges have stabilized for a given molar volume of the cluster, we allow symmetric small ( $\Delta = 0.1-0.2$  Å) relaxations of the lattice around the guest molecule, in directions parallel to the body diagonals of the  $Pa3$  unit cell, in order to examine the effect of model distortions on the defect states.

### 1. Hydrogen atom impurity

Table 1 summarizes the main results obtained for the H atom defect.

The energy of the impurity states is shown to become stable relative to the band edges, resulting in a net destabilization of the atomic  $1s$  state of hydrogen relative to the free atom. The one-electron energy state corresponding to hydrogen impurity is highly localized in the vicinity of the atom, exerting only small perturbation on the charge distribution of the neighbouring molecules. The guest atom acts as a slight charge acceptor, and accumulates a net electron density on it of the order of  $-0.02e$ . Inward relaxations of the lattice result in a relative destabilization effect on the defect state, while outward relaxation tend to stabilize it. It should, however, be kept in mind that the cluster model suggested does not represent adequately the real restoring forces of the covalent molecular crystal due to the lack of second order polarization forces in this closed shell LCAO picture. Calculations of equilibrium positions of the surrounding molecules are therefore not possible.

As the unit cell dimension of the crystal is decreased, (Fig. 5) the impurity level approaches the edge of the conduction band being for instance, already  $8.7$  eV from it at  $a = 5.0$  Å. The net charge accumulated on the defect atom rises also with decreasing unit cell dimension, and becomes  $-0.041e$  for  $a = 5.0$  Å. The ionization potential of the crystal increases by  $0.02$  eV on the average, due to the presence of the defect atom.

### 2. Nitrogen molecule impurity

An isolated  $N_2$  molecule is described in the IEXH frame (free atom orbital energies taken from Hartree-Fock calculation on the  $^4S$  ground state[51] and charge dependent energies from the work of Rein *et al.*[22]) to have an equilibrium internuclear distance of  $1.15$  Å (experimental value  $1.098$ [26]) a  $2\sigma_g$  ionization potential of  $16.10$  eV (experimental value  $15.60$  eV[52]), a dissociation energy of  $9.9$  eV (experimental value  $9.756$  eV[26]) and a bond population of  $1.675$ . The lowest vacant orbital is a doubly degenerate  $\pi_g$  orbital at  $11.1$  eV. The  $N_2$  molecule is placed at the origin of the  $Pa3$  molecular hydrogen cluster and calculation steps (a)–(c) performed. The results are shown in Table 2.

The  $\pi_g$  orbital remains unsplit in the crystal and appears in the band gap. The lowest  $2\sigma_g \rightarrow \pi_g$  molecular transition is blue shifted relative to the transition in the isolated molecule by  $0.18$  eV at normal density. Both  $2\sigma_g$  and the  $\pi_g$  levels are stabilized in the crystal relative to their free molecule positions while smaller stabilizing effects are manifested in the inner  $2\sigma_g$ ,  $2\sigma_u$  and  $\pi_u$  molecular orbital energies.

Again the guest molecule has only a small perturbative effect on the charge distribution around it, at normal density, and the nitrogen molecular bond population decreases slightly with respect to the free molecule value. As the density of the cluster is increased, the defect  $\pi_g$  level exhibits only small changes under compression of the crystal (Fig. 5) and the charge on each nitrogen atoms

Table 1. Energy states of conduction and valence band edges and impurity state for relaxed ( $\Delta = 0.2$  Å) and unrelaxed lattice for the H-impurity clusters

Cluster	Conduction edge (eV)	Valence edge (eV)	Impurity state (eV)		
			No relaxation	Inward relaxation	Outward relaxation
I + 36	4.451	15.098	13.419	13.398	13.578
I + 42	4.455	15.065	13.418	13.399	13.580
I - 54	4.456	15.065	13.417	13.399	13.580
I + 76	4.456	15.063	13.417	13.399	13.580

Table 2. Energy states of conduction and valence band edges and impurity state for relaxed ( $\Delta = 0.2$  Å) and unrelaxed lattice for the  $N_2$  impurity clusters

Cluster	Conduction edge (eV)	Valence edge (eV)	$\pi_g$ Impurity state (eV)		
			No relaxation	Inward relaxation	Outward relaxation
I + 36	4.447	15.094	11.099	11.030	12.050
I + 42	4.455	15.066	11.098	11.032	12.052
I + 54	4.456	15.065	11.098	11.033	12.054
I + 76	4.456	15.065	11.098	11.034	12.054

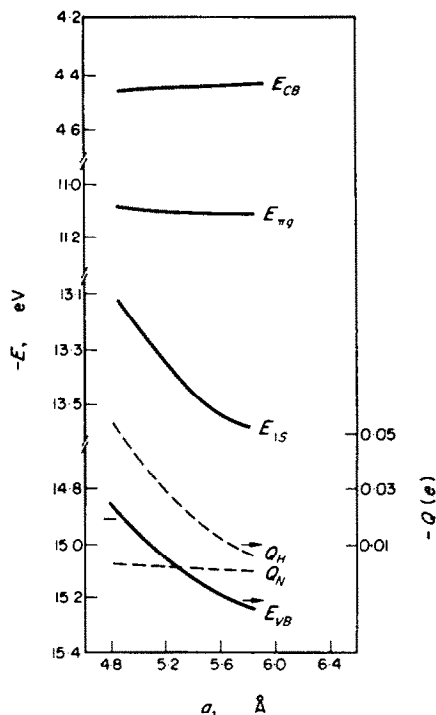


Fig. 5. Variation of some electronic properties for the defect crystal problem.  $E_{CB}$  and  $E_{VB}$ : energies of the edge of conduction and valence bands respectively (with  $N_2$  impurity).  $E_{\pi\sigma}$ : one electron defect state of  $N_2\pi_\sigma$  level,  $E_{1S}$ : one electron defect state of H 1S level  $Q_H$ ,  $Q_N$ : net atomic charges of H and N atoms in the cluster.

increases slightly in absolute value, on expense of the less electronegative hydrogen molecules surrounding it. Relaxation of the lattice around the impurity molecule results in relatively small shifts of the impurity level.

## 6. SUMMARY

We have used the truncated crystal approach with an approximate LCAO method to calculate the convergence limit of the ionization potential, energy gap and transition density of states of molecular hydrogen clusters, for several densities, as a function of cluster size for "spherical" clusters. Information regarding density effects on charge distribution and one electron energy levels is obtained via a charge self consistent model. The Exciton states of the lowest molecular excited state in the ideal crystal and model impurity states due to hydrogen atom and nitrogen molecule, are investigated. The main advantages of the method lie in its ability to treat ideal crystal states as well as localized defect states in a unified model when the convergence limit is reached and in the simple way of introducing self-consistent charge redistribution and relaxation effects. The main shortcomings of the proposed model are the limited basis set used and the

lack of configuration interaction in the calculation, which are both presently excluded due to limitation in computer storage.

**Acknowledgements**—The author would like to thank Prof. J. Jortner for many helpful discussions and advice. Professor R. Engelman is gratefully acknowledged for critical reading of the manuscript.

## REFERENCES

- Moore E. B. and Carlson C. M., *Solid State Commun.* **4**, 47 (1965).
- Larkins F. P., *J. Phys. Chem.* **4**, 3065, 3077 (1971).
- Zunger A., *Solid State Commun.* **11**, 1717 (1972).
- Messmer R. P. and Watkins G. D., *Phys. Rev. Lett.* **25**, 656 (1970); *Phys. Rev.* **B7**, 2568 (1973).
- Zunger A., *J. Phys. C* (a) **7**, 76 (1974), (b) **7**, 96 (1974).
- Hayns M. R., *Phys. Rev.* **B5**, 697 (1972), also *J. phys. Chem.* **5**, 15 (1972).
- Johnson K. H., *J. de Phys.* **C3**, 195 (1972).
- Watkins G. D. and Messmer R. P., in *Computational methods for large molecules and localized states in solids* (edited by Herman F., McLean A. D. and Nesbet R. K.) p. 133. Plenum Press, New York (1973).
- Messmer R. P. and Watkins G. D., in *Radiation damage and defects in semiconductors*, Conference Series No. 16, p. 255. The Institute of Physics, London (1973).
- Koster G. F. and Slater J. C., *Phys. Rev.* **95**, 1167 (1954).
- Coulson C. A. and Kearsley M. J., *Proc. R. Soc. Lond.* **A241**, 433 (1957).
- Dynin E. A., *Sov. Phys. Solid State* **13**, 2089 (1972).
- Chapline G. F., *Phys. Rev.* **B6**, 2067 (1972).
- Neece G. A., Rogers F. J. and Hoover W. G., *J. Computational Phys.* **7**, 621 (1971).
- Basov N. G., Krokhin O. and Sklizkev G. V., *Proc. 2nd W.S. at Renssel Poly. Inst. Hartford*, p. 389 (1971).
- Bruce T. A., *Phys. Rev.* **B5**, 4170 (1972).
- Krumhansl J. A. and Wu S. Y., *Phys. Rev.* **B5**, 4155 (1972).
- McGinty D. J., *J. chem. Phys.* **55**, 580 (1971).
- Burton J. J., *J. chem. Phys.* **52**, 345 (1970).
- Zunger A., *Mol. Phys.* **28**, 713 (1974).
- Cusachs L. C. and Reynolds J. W., *J. chem. Phys.* **43**, S160 (1965).
- Rein R., Fukuda H., Win H., Clark G. A. and Harris F. E., *Quantum aspects of heterocyclic compounds in chemistry and biochemistry*, p. 86, Proc. of Jerusalem Symposium, Israel Academy of Science and Humanities (1969).
- Pople J. A., Beveridge D. L., *Approximate M.O. theory*, McGraw-Hill, New York (1970).
- Blyholder G. and Coulson C. A., *Theor. Chim. Acta.* **10**, 316 (1968).
- Gilbert T. L., *Sigma molecular orbital theory* (edited by Sinnanoglu O. and Wibery R.), p. 249, Yale University Press. (1970).
- Herzberg G., *Diatom molecules*, University Press, Van Nostrand, Princeton, New Jersey (1950).
- Roothaan C. C. J., *J. chem. Phys.* **19**, 1445 (1951).
- Zunger A., unpublished.
- Baldini G., *Jap. J. App. Phys.* **4**, Suppl. I. 613 (1965).
- Margenuu H. and Kestner N. R., *Theory of intermolecular forces*, Pergamon Press, Appendix A (1969).
- Salem L., *J. Amer. chem. Soc.* **90**, 543 (1968).
- Michels A. M., de Graaf W. and ten Seldam C. A., *Physica* **26**, 393 (1960).

33. Alder B. J., Christian R. M., *Phys. Rev. Lett.* **4**, 450 (1960).  
 34. Raich J. C., *J. chem. Phys.* **45**, 2673 (1966).  
 35. Schmidt L., *Phys. Lett.* **36a**, 87 (1971).  
 36. Hexter R. M., *J. chem. Phys.* **36**, 2285 (1962).  
 37. Nijboer B. R. A. and de Wette F. W., *Physica* **24**, 422 (1958); *ibid.* **24**, 1105 (1958).  
 38. Hexter R. M., *J. chem. Phys.* **37**, 1347 (1962).  
 39. Geiger J. and Tropschowsky M., *Z. Naturforsch.* **21a**, 626 (1966).  
 40. Jarmain W. R., Ebisvzaki R. and Nichollas R. W., *Can. J. Phys.* **38**, 510 (1960).  
 41. Brith M. and Schnepf O., *Mol. Phys.* **9**, 473 (1965).  
 42. Gedanken A., Raz B. and Jortner J., *Chem. Phys. Lett.* **14**, 326 (1972).  
 43. Gedanken A., Raz B. and Jortner J., *J. chem. Phys.* **59**, 2752 (1973).  
 44. Raz B. and Jortner J., *Chem. Phys. Lett.* **4**, 155 (1969).  
 45. Mott N. F. and Littleton M. J., *Trans. Faraday. Soc.* **34**, 485 (1938).  
 46. Springett B. E., Cohen M. H. and Jortner J., *J. chem. Phys.* **48**, 2720 (1968), *ibid.* **51**, 2291 (1969).  
 47. Halpern B. and Gomer R., *J. chem. Phys.* **51**, 1031 (1969).  
 48. Bobin J. and Tonon G. F., *IV Europ. conf. controll. fusion*, p. 1 (1970).  
 49. Bebb H. B. and Gold A., *Phys. Rev.* **143**, 1 (1966).  
 50. Mennicke H., *Phys. Lett.* **37a**, 381 (1971).  
 51. Clementi E., *IBM J. Res. Develop. Suppl.* **9**, 2 (1965).  
 52. Cederbaum L. S., Hohlnei G., and Von Niessen W., *J. chem. Phys.* **44**, 1973 (1966).

*Note added in proof*

After this paper has been accepted, two papers on the band structure of solid  $Pa_3$  Hydrogen have appeared: the work of L. A. Gomez, G. P. Parravicini, L. Resca and R. Resta [*J. Phys. C*, **6**, 1926 (1973)] using a tight-binding procedure with nearest-neighbor interactions, neglecting three and multicenter integrals and employing a Slater 1s minimal set, and the simplified KKR calculations of R. Monnier, E. L. Pollock and C. F. Friedli [*J. Phys. C*, **7**, 2467 (1974)] using a spherical approximation to the Columb molecular potential including three forms of exchange (Slater<sup>(a)</sup>, Lundqvist-Lundqvist<sup>(b)</sup> and Khon-Sham<sup>(c)</sup>) in a non-self-consistent treatment. The following table summarizes the results:

Property	Monnier <i>et al.</i>	Gomez <i>et al.</i>	Present work	Expt.
IP (solid) eV	19.1 <sup>(a)</sup> 15.5 <sup>(b)</sup> 14.2 <sup>(c)</sup>	15.82	15.1	14.5 <sup>(f)</sup>
Band width eV	0.369 <sup>(a)</sup> 0.825 <sup>(b)</sup> 0.945 <sup>(c)</sup>	1.1	1.22	—
E <sub>g</sub> eV	12.029 <sup>(a)</sup> 9.276 <sup>(b)</sup> 8.789 <sup>(c)</sup>	—	10.7	~10.8 <sup>(d)</sup>
IP (molecule) eV	15.0	16.135	15.38	15.43 <sup>(e)</sup>
Dissociation Energy (molecule) eV	3.488	3.488	4.66	4.474 <sup>(e)</sup>

(a) Slater exchange [J. C. Slater, *Phys. Rev.* **81**, 385 (1951)].

(b) Lundqvist-Lundqvist exchange [B. I. Lundqvist and S. Lundqvist, *Computational Solid State Physics* (Edited by F. Herman, N. W. Dalton and T. R. Koehler) p. 219. Plenum, New York (1972)].

(c) Kohn and Sham exchange [W. Khon and L. J. Sham, *Phys. Rev.* **140A**, 1133 (1965)].

(d) Ref. 29.

(e) Ref. 26.

(f) Ref. 43.

In this table, IP (solid) denotes the negative of the highest occupied valence band state ( $\Gamma_4$  in the notation of Gomez *et al.* and  $X_1$  in the notation of Monnier *et al.*) and  $E_g$  denotes the transition between the  $\Gamma_4$  and  $\Gamma'_4$  states ( $X_1 \rightarrow X_4$  in the notation of Monnier and  $T_g \rightarrow T'_g$  in the notation of the present paper). The Lundqvist-Lundqvist local exchange correlation<sup>(b)</sup> is argued by Monnier *et al.* to be the 'best' one judging from the properties of the free molecule. Reasonably good agreement is obtained between the present work and the works of Gomez *et al.* and Monnier *et al.* In a recent OPW calculation for the conduction bands of solid  $H_2$  [G. P.

Parravicini and M. Vittori, unpublished], using a nonlocal exchange potential in the zero-overlap approximation and a Coulomb potential from the Slater 1s charge density, the lowest conduction state was calculated to be of  $\Gamma_1$  symmetry and this state was separated by a gap of 13.8 eV from the top of the valence band. The energy of the first allowed transition was calculated to be 16.3 eV in contrast with the work of Monnier *et al.* ( $E_g > 9.28$  eV), the present work ( $E_g = 10.7$  eV) and the observed edge of the absorption edge of Baldini, 10.8 eV [29].